# Comparison of alternative methodologies for identifying and characterizing preferential flow paths in heterogeneous aquifers

Le Borgne, T; Bour, O; Riley, Michael; Gouze, P; Belgouhl, A; Lods, G; Le Provost, R; Greswell, Richard; Ellis, PA; Isakov, E; Last, Brian; Pezard, PJ

*DOI:*
10.1016/j.jhydrol.2007.07.007

*Document Version*
Publisher's PDF, also known as Version of record

*Citation for published version (Harvard):*
Le Borgne, T, Bour, O, Riley, M, Gouze, P, Belgouhl, A, Lods, G, Le Provost, R, Greswell, R, Ellis, PA, Isakov, E, Last, B & Pezard, PJ 2007, 'Comparison of alternative methodologies for identifying and characterizing preferential flow paths in heterogeneous aquifers', *Journal of Hydrology*, vol. 345, no. 3-4, pp. 134-148. https://doi.org/10.1016/j.jhydrol.2007.07.007

Journal of Hydrology (2007) 345, 134–148

available at www.sciencedirect.com

ScienceDirect

journal homepage: www.elsevier.com/locate/jhydrol

# Comparison of alternative methodologies for identifying and characterizing preferential flow paths in heterogeneous aquifers

T. Le Borgne [b,*], O. Bour [b], M.S. Riley [c], P. Gouze [a], P.A. Pezard [a], A. Belghoul [a], G. Lods [a], R. Le Provost [a], R.B. Greswell [c], P.A. Ellis [c], E. Isakov [c], B.J. Last [c]

[a] *Géosciences Montpellier (Université de Montpellier 2, UMR CNRS 5243), Montpellier, France*
[b] *Géosciences Rennes (UMR CNRS 6118), University of Rennes, Rennes, France*
[c] *Hydrogeology Research Group, School of Geography, Earth and Environmental Sciences, University of Birmingham, Edgbaston, Birmingham B15 2TT, UK*

Received 29 May 2006; received in revised form 9 July 2007; accepted 11 July 2007

**KEYWORDS**
Fracture;
Connectivity;
Flowmeter;
Packer;
Geophysical measurements

**Summary** One of the main difficulties encountered when characterizing the hydrodynamic properties of a fractured aquifer is to identify the preferential flow paths within it. Different methods may be applied to determine the variability of the permeability at the borehole scale and to image the structure of the main flow zones between boreholes. In this paper, we compare the information obtained from different measurement techniques performed in a set of three 100 m depth wells (well-to-well spacing: 5–10 m) in a fractured crystalline rock setting. Geophysical logging and borehole-wall imaging are used to identify open and closed fractures intersecting the boreholes and their orientation. The comparison with flowmeter and single packer tests shows that few of the fractures interpreted as open from geophysical logs are significantly transmissive. Cross-borehole connectivity is first investigated from single packer tests with pressure monitoring in adjacent boreholes. To determine fracture zone connectivity, we propose a methodology simply based on the variation with packer depth of the ratio of the drawdown in the observation well and the drawdown in the pumping well. The results are compared to the analysis of cross-borehole flowmeter tests. We show that both methods provide consistent results with a similar level of information on connectivity.


* Corresponding author. Tel.: +33 2 23 23 67 02.
*E-mail address:* tanguy.le-borgne@univ-rennes1.fr (T. Le Borgne).

0022-1694/$ - see front matter © 2007 Elsevier B.V. All rights reserved.
doi:10.1016/j.jhydrol.2007.07.007

## Introduction

In fractured rock, flow is often localized in a few main flow paths that control most of the hydrological response of the aquifer. The identification of these main flow paths is critical since it controls the transfer of fluid as well as the transport of solutes in the subsurface. In particular, the spatial organization of these flow paths controls the dependence of hydraulic properties on scale (Sanchez-Vila et al., 1996; Bour and Davy, 1997; Hsieh, 1998; de Dreuzy et al., 2001a; Illman, 2006; Le Borgne et al., 2004; Le Borgne et al., 2006a,b). However, information about the connectivity of theses main flow paths — e.g. about the connectivity of the most transmissive fractures in the rock mass — is generally very difficult to obtain. It usually requires the identification of the most transmissive features at the borehole scale followed by intensive double packer testing between boreholes with monitoring of pressure variations in multiple intervals in observation boreholes (Butler et al., 1999; Day-Lewis et al., 2000; Muldoon and Bradbury, 2005; Martinez-Landa and Carrera, 2006). The interpretation of such hydraulic tests has been largely improved in the last few years through numerous works about hydraulic tomography (Butler et al., 1999; Yeh and Liu, 2000). However, this method is time consuming and requires instrumental resources that are rarely available for systematic use. As a result, information about the connectivity of the main flow paths or about the connectivity of the most transmissive fractures is not available in most hydrogeological sites. Recently, an alternative method has been proposed to obtain the same kind of information through flowmeter tests (Williams and Paillet, 2002), which have the great advantage that they do not require the use of packers.

In this paper, we compare the information that may be derived from different field techniques including geophysical and imaging logs, single and cross-borehole flowmeter tests (Williams and Paillet, 2002), and single and double packer tests (Day-Lewis et al., 2000; Karasaki et al., 2000). Our results are based on a field study at the Plœmeur crystalline aquifer, in Britanny, France. On the main pumping site, an average of 2000 l/min is pumped from a set of three wells for the supply of drinking water for the town of Plœmeur. The large scale transmissivity is on the order of $10^{-3}$ $m^2/s$, which is high compared with that generally expected in similar rocks in Brittany. Flow is localized in a few fractures zones, whose width does not exceed a few meters. The good fracture network connectivity is thought to be related to the existence of a sub-horizontal contact between the intrusive granite and the overlying mica-schist (Le Borgne et al., 2004; Le Borgne et al., 2006b). The present study is focused on the Stang er Brune site, located about 3 km west of the main pumping site (Fig. 1), in similar geological conditions, at the contact between the Plœmeur granite with the overlying micaschistes. This experi-

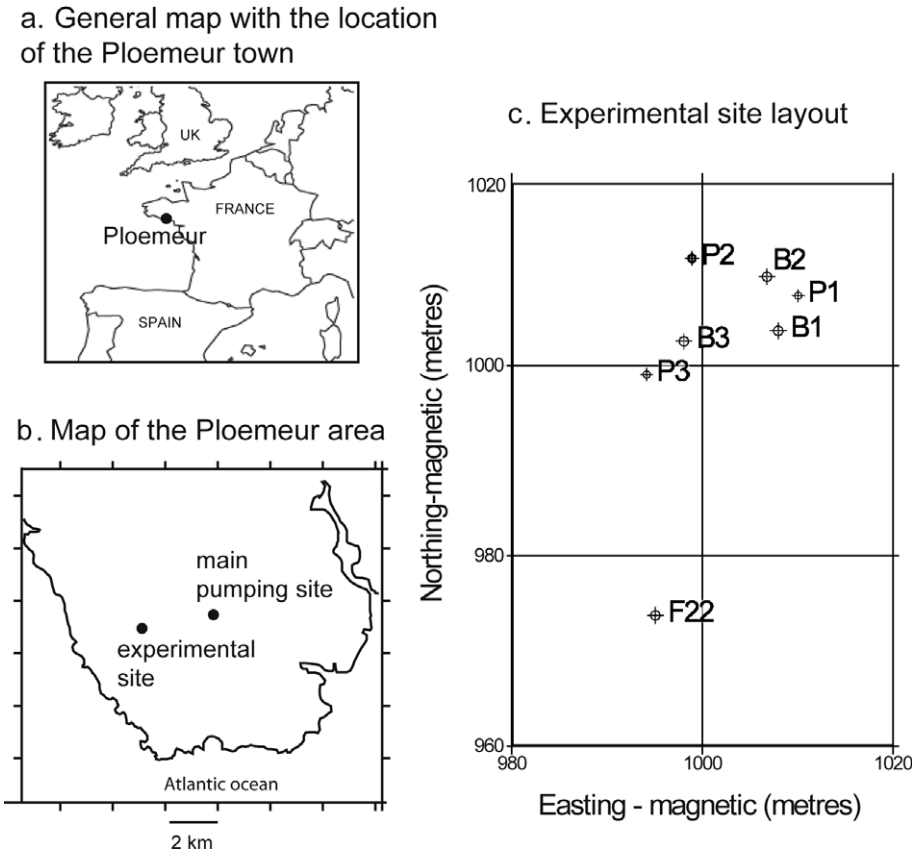


**Figure 1** Location of the experimental site. (a) General map with the location of the Ploemeur town, (b) map of the Ploemeur area and (c) experimental site layout. Boreholes B2 and B3 are 100 m deep. The cored borehole B1 is 84 m deep. Borehole F22 is 70 m deep. Boreholes P1, P2 and P3 are shallow, 10 m deep piezometers.

mental site was set up as part of the European projects ALIANCE and SALTRANS and is now part of the Observatory for Environmental Research H+. The site is composed of (i) three unscreened wells of 80—100 m depth forming a triangle of size about 10 m (wells B1, B2, B3), including one fully cored borehole (B1), (ii) a well (F22) of 70 m depth, positioned at about 35 m from the B1—B3 hydropad and (iii) three shallow, 10 m deep piezometers used to monitor water level in the superficial weathered crystalline zone. Beneath the new borehole array, mica schist overlies the Plœmeur Granite at a depth of approximately 40 m. The overall transmissivity, derived from hydraulic tests in each well varies around $10^{-3}$ $m^2/s$.

We focus our analysis on the identification of the main flow paths at the borehole scale and between boreholes. Our main goal is to provide a comparison of different methodologies that can be used for characterizing preferential flow paths in heterogeneous systems at the site scale.

## Identification of transmissive fractures

### Characterization of open fractures from geophysical and optical logs

Borehole geophysical measurements (e.g. electrical resistivity log) along with imaging, cores, and thin-section analyses can be combined to obtain a detailed characterization of fractures in terms of geometry and origin (Pezard and Luthi, 1988; Genter et al., 1997). Note that in the term *geophysical measurements* we do not include flowmeter logs that are described in a following section. Eletrical resistivity

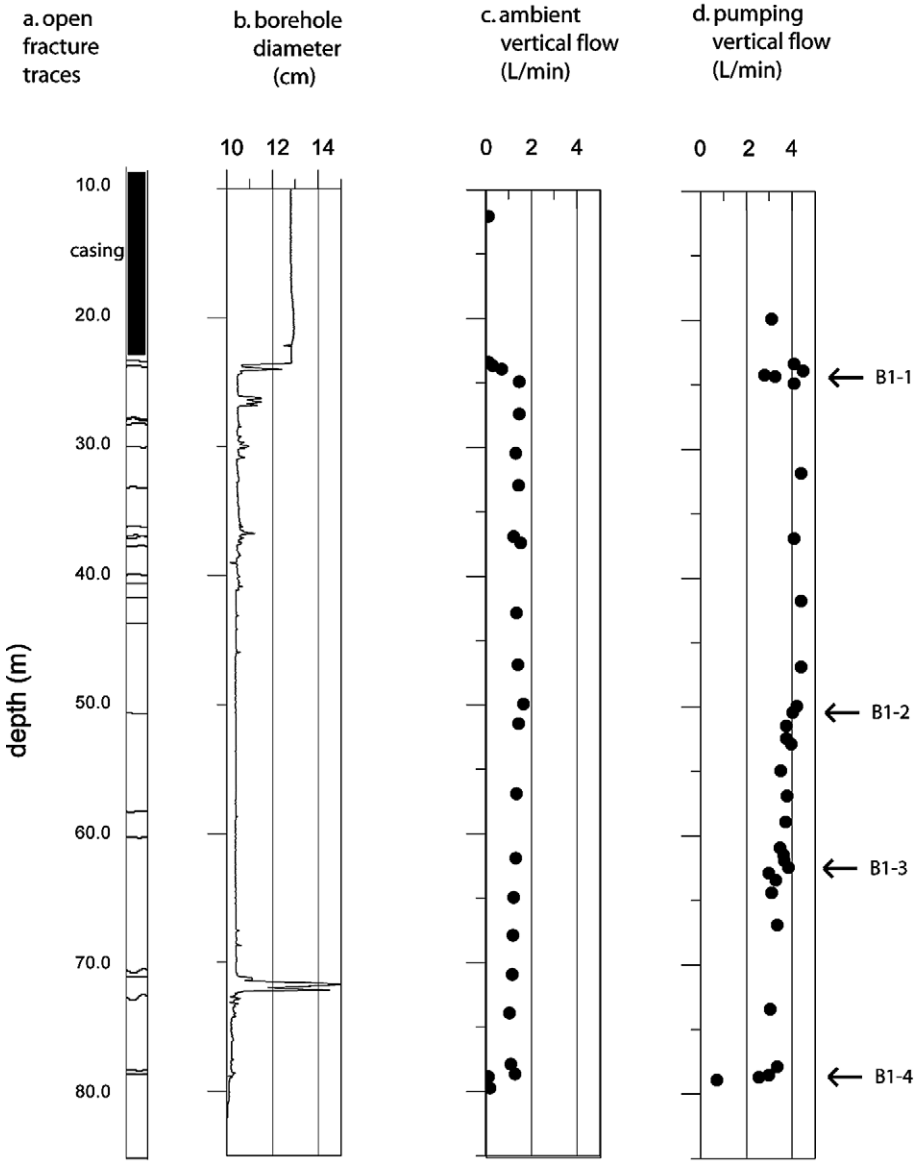


**Figure 2** Geophysical and flowmeter logs in borehole B1. (a) Fracture traces measured on optical and acoustic logs. Only the fractures interpreted as open from the image logs are represented, (b) caliper log, (c) ambient vertical velocity (positive values correspond to upflow) and (d) vertical velocity measured while pumping in the cased part of the well at a rate of 3 l/min. The steady state drawdown observed was 6 cm.

can be used to identify open fractures since a decrease of the electrical resistivity with respect to the surrounding matrix is obtained in front of an open fracture. However, such a decrease can be due solely to the presence of clays in the fracture. An electrical resistivity decrease is therefore not sufficient to identify an open fracture. From the optical and acoustic image logs, open fractures that cross the borehole may be identified and differentiated from fractures filled either with clays, quartz or chlorite. Acoustic and optical imaging in the borehole yield continuous and oriented 360° views of the borehole wall at the mm- to cm-scale (Fig. 2). In map view, the fractures are characterized by sinusoid traces, either complete or partial. This representation corresponds to unfolding the borehole surface onto a plane. The dip and dip direction of fractures are measured from each of the sinusoids. The local aperture of fractures may be characterized from a local increase in acoustic transit time data along the trace. Fig. 2(a) shows the fractures identified as open for borehole B1 from the joint interpretation of optic, acoustic and electrical logs. Note that fractures that appear as open in the borehole wall are not necessarily transmissive since they may be closed or filled in the vicinity of the borehole. These results are synthetized for all boreholes in Tables 1—3.

## Single packer tests

A reconnaissance survey was conducted at the site using single packer equipment to identify the major transmissive zones and to investigate the magnitude of non-linear energy losses within pumped fractures (see e.g. Lloyd et al., 1996; Kolditz, 2001; Qian et al., 2005). Measurements were made by inflating a packer at a given depth and performing a step drawdown test using a pump located above the packer. The pressure response was monitored in the sections above and below the packer and in all other boreholes. In general, the observed drawdown in the pumped zone decreases with increasing packer depth, as the number of transmissive fractures intersected increases. The changes in drawdown at successive packer depths can be used to identify transmissive regions, which in conjunction with the optical and acoustic borehole logs can highlight the probable locations

**Table 1** Flow zones depths below top of casing in borehole B1 deduced from single borehole flowmeter and single packer tests

| Fracture zone number | Optic/acoustic | Single packer test | Flowmeter test | Dip direction | Dip angle |
|---|---|---|---|---|---|
| B1-1 | 24.10 m weak trace | | 24.05 ± 0.1 | 317° | 40° |
| B1-2 | 50.90 m open | Between 52.1 and 46.5 m | 50.40 ± 0.5 | 228° | 37° |
| B1-3 | 60.9 m open | Between 62 and 53.1 m | | 220° | 31° |
| | 63.4 m no signal | | 62.60 ± 0.3 | 281° | 81° |
| B1-4 | 78.70 m open | Below 74 m | 78.70 ± 0.1 | 215° | 15° |

Comparison with optic and acoustic log and ambient flow measured.

**Table 2** Flow zones depths below top of casing in borehole B2 deduced from borehole flowmeter and single packer tests

| Fracture zone number | Optic/acoustic | Single packer test | Flowmeter test | Dip direction | Dip angle |
|---|---|---|---|---|---|
| B2-1 | Casing | | 25.4 ± 0.4 | | |
| | 27.85 m open | | 27.4 ± 0.2 | 305° | 42° |
| B2-2 | 55.60 m open | Between 57.95 and 52.3 m | 55.90 ± 0.5 | 213° | 33° |
| B2-3 | 58.85 m open | Between 71.5 and 59.45 m | 58.60 ± 0.3 | 191° | 31° |
| B2-4 | 79.30 m 79.50 m weak trace | | 79.10 ± 0.2 | 270° | 72° |
| | 81.5 m weak trace | Between 81.07 and 71.5 m | | 104° | 45° |
| B2-5 | 97.5 m open | Below 84 m | 97 ± 0.1 | 102° | 53° |
| | 97.6 m weak trace | | 96.60 ± 0.1 | 100° | 51° |
| | 98.5 m open | | 98.5 ± 0.1 | 288° | 59° |
| | 99.1 m weak trace | | 98.91 ± 0.1 | 309° | 58° |

Comparison with optic and acoustic log.

**Table 3** Flow zones depths below top of casing in borehole B3 deduced from single borehole flowmeter and single packer tests

| Fracture zone number | Optic/acoustic | Single packer test | Flowmeter test | Dip direction | Dip angle |
|---|---|---|---|---|---|
| B3-1 | 2 open fractures from 36.2 to 37.2 m | Above 41.5 m | 37.5 ± 0.5 | 342° | 84° |
| B3-2 | Open fracture at 44.90 m | Between 48 and 42.5 m | 45 ± 1.0 | 254° | 52° |
| B3-3 | 3 fractures 2 of which are steeply dipping from 79.90 to 81.7 m | Between 83 and 80.1 m | 80.4 ± 0.5 | 0° | 71° |

Comparison with optic and acoustic log.

of fractures that transmit water. For this study, the drawdown at the end of the first pumping step has been used in the analysis, since non-linear losses are minimal and steady state is clearly achieved. Employing the same pumping regime at each depth is not essential, but allows direct identification of changes in transmissivity.

Assuming non-linear losses in fractures to be negligible, the relationship between the steady state drawdown, $s_B$, in a borehole ($B$) and the constant pumping rate, $Q$, can be characterized by a conductance, $C_B$ [$L^2T^{-1}$], given by

$$C_B = \frac{Q}{s_B} \quad (1)$$

(e.g. Sanford et al., 2006; Dershowitz and Fidelibus, 1999). If flow to $B$ is considered two-dimensional and radially symmetric, the effective homogeneous transmissivity of the region around the borehole is related to the conductance using the Thiem analysis by

$$T_B = \frac{C_B}{2\pi} \ln\left(\frac{R_B}{r_w}\right), \quad (2)$$

where $r_w$ is the radius and $R_B$ the radius of influence of borehole $B$.

The locations of the most transmissive zones inferred from the tests (Fig. 3) are reported in Tables 1–3. Decreasing drawdown with packer depth is not always observed. For example, B2 contains open fractures at 55.65 and 58.85 m but pumping from above the packer located between the two fractures produces less drawdown than when the packer is lowered to 60.5 m. However, repeating the test with the fracture at 58.85 m blocked by the packer produces drawdown consistent with increasing transmissivity with depth. It is concluded that the fracture at 55.65 m is well connected with that at 58.85 m, which if left unblocked, provides a good hydraulic connection to the full depth of the borehole producing an apparently large effective transmissivity in the 55.65 m fracture and above. Thus, the possibility of short-circuiting a simple single packer demands that results from the application of simple, single packer systems be considered carefully. However, in appropriate circumstances, judicious packer placement can provide information on vertical connections in the system.

## Single borehole flowmeter tests

High-resolution borehole flowmeters such as the heat-pulse flowmeter (Hess, 1986) can also be used to identify flow zones such as fractures intersecting boreholes. Ambient vertical borehole flow from one fracture zone to another is commonly observed, due to differences in hydraulic head between large-scale flow paths that connect to fractures intersecting boreholes. These differences in hydraulic head may be due to the global flow direction: downwards in recharge areas and upwards in discharge areas. To estimate the hydraulic heads and local transmissivities, single-borehole flowmeter tests need to be performed under two different flow conditions, usually ambient and pumping conditions (Paillet, 1998, 2000).

At the Stang er Brune site, borehole flows were first measured in ambient conditions in the four boreholes using a heat-pulse flowmeter (Fig. 2c). The flowmeter was equipped with a 10 cm diameter flow concentrator that acts to focus the main part of the flow in the measuring zone, in order to increase the sensitivity of the tool. For each borehole, a second borehole flow profile was obtained while pumping at pumping rates ranging between 3 l/min and about 20 l/min depending on the well. Flowmeter output gives the mean travel time of the heat pulse mode moving from the heating grid to the thermistors located 5 cm above and below the heat source within the cylindrical measurement section. The vertical flow is estimated from these velocity measurements using a flow calibration performed in the borehole above all flow zones (Paillet, 2004). Flow profiles are then obtained from flowmeter measurements with the flowmeter positioned at different depths (Fig. 2). The flow profiles are measured in ambient condition and in pumping condition, with a pump placed at the top of the well.

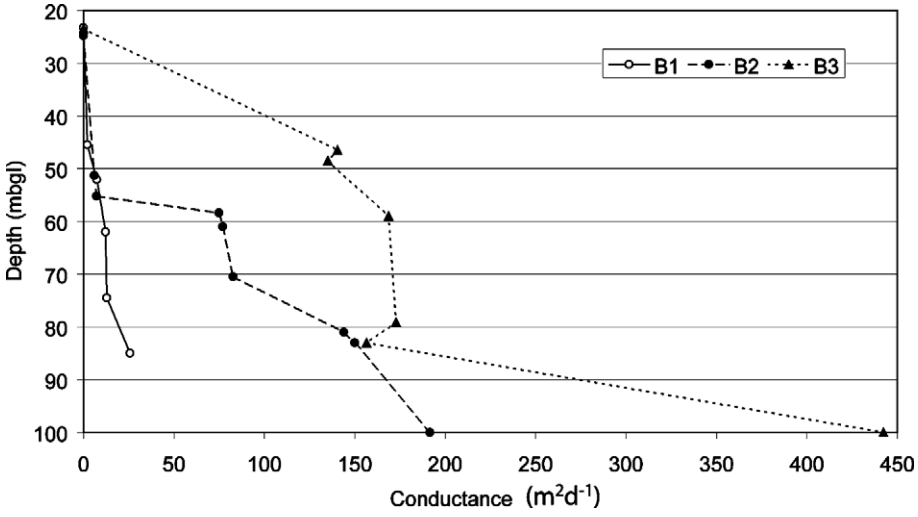


**Figure 3** The cumulative conductance with depth in boreholes B1, B2 and B3 derived from single packer tests. Markers indicate the bottom of the packered zone in the pumped borehole. The top marker for each borehole indicates the location of the bottom of the casing.

Inflow points for each observation borehole were identified by inspection of the pairs of ambient and pumping flow profiles. Note that, as discussed by Paillet (2004), there is an inherent variability in flowmeter measurement. Scatter in flow measurements is related to the variability in the coaxiality of the flowmeter and the borehole. Hence, the permeability detection capability of flowmeters is effectively limited to about two orders of magnitude regardless of their dynamic range and accuracy. Therefore, flowmeter tests may be used to characterize the main flow zones within boreholes. Ambient upflow was measured in all boreholes. Inflow zones are deduced from changes in the measured vertical flow (Fig. 2). In Tables 1–3, the locations of transmissive zones are reported with an estimate of the vertical resolution that corresponds to the spacing between flow measurement stations.

### Comparison of the different single-borehole techniques

For further reference in the text, the fracture zones in each borehole are numbered (see Tables 1–3). Few of the fractures interpreted as open from geophysical logs contribute significantly to flow. Similar results were also obtained at other sites (Paillet, 1993; Nativ et al., 2003; Hitchmough et al., 2007). Some fractures may appear open in the vicinity of the borehole whereas they are actually closed. Often, the transmissive zones may be associated unambiguously with fractures interpreted as open from optical and acoustic image logs (Fig. 2). However, in a few occurrences, the transmissive zones correspond to weak traces on the optic and acoustic logs. In general, we observed that flowmeter and hydraulic tests using single packer give coherent results in term of transmissive zone localization (Tables 1–3). Both methods are based on cumulative measurements. The flowmeter test accuracy is lower at the top of the well, right under the pump, since the flowmeter measures the contribution of all flow zones in the borehole. On the other hand, the single packer test accuracy is lower when located at the bottom of the well, since the pressure response measured is that of all the fractures in the well.

## Connectivity of transmissive fractures

In this section, we compare different methods to derive the cross-borehole connectivity of transmissive fractures. These methods include: (i) projecting the intersection of transmissive fractures with other boreholes, using the estimates of fracture strike and dip determined from geophysical logs; (ii) single packer hydraulic tests with pressure monitoring in adjacent wells; (iii) cross-borehole flowmeter tests, performed by turning on a pump in one of the wells, while tracking measurable changes in vertical flow in the other boreholes; (iv) multi-level pressure monitoring in observation wells during hydraulic tests. Although some quantitative results are presented, we focus the analysis on a qualitative characterization of fracture connectivity. We do not quantify a degree of connectivity. The main point is to compare the methods in terms of characterization of the geometry of the connected fractures.

### Three-dimensional geometry of transmissive fractures

To define the connections between boreholes, one may argue that the simplest solution consists of projecting the intersection of transmissive fractures with other boreholes, using the estimates of fracture strike and dip determined from geophysical logs. Some of the transmissive fracture orientations are found in several boreholes (Tables 1–3). For instance, the B1-1 and B2-1 fracture zones have similar orientations. Also the B1-2, B1-3 and B2-2, B2-3 zones have similar orientations. On the other hand, the fracture zone orientations in B3 and in F22 are not found in other boreholes.

Fig. 4 represents the geometry of transmissive fractures for two pairs of boreholes. The geometry of the boreholes in space was determined from multi-directional magnetometers. We observe that the B1-1 and B2-1 fracture zones could form a continuous fracture zone. Conversely, the B2-2, B2-3 zones do not intersect the B1 borehole at the same depth as the B1-2 and B1-3 zones. Note that there are some uncertainties in the precise estimation of the dip direction and angle since they are measured over the borehole cross-section, which is relatively small. Despite these uncertainties it is found that most transmissive fractures are not continuous between boreholes. It suggests that the transmissive fractures in one borehole are either closed in other boreholes or have been shifted. The hydraulic connections between boreholes are thus likely formed through complex three-dimensional patterns of fractures.

### Single packer hydraulic tests with pressure monitoring in adjacent boreholes

The interpretation of single well packer tests with pressure monitoring in adjacent wells, in fractured media, is very specific compared to the interpretation of regular hydraulic tests. To interpret this kind of test correctly in terms of fracture connectivity it is essential to account for vertical flows that occur between fractures in boreholes. In the following, we express the hydraulic properties of the connecting zones in terms of conductances and we show that the key parameter to assess fracture connectivity from one borehole to another using single well-packer tests is the ratio of the drawdown in observation wells to the drawdown in the pumping well $s_{obs}/s_{pump}$ for different packer positions in the pumping well. Then, we interpret the single packer test dataset using this method.

#### Characterization of preferential flow paths connectivity from single packer tests

In terms of steady state, linear flows, the hydraulic connections between the section of a pumping borehole ($A$) above the packer and an observation borehole ($B$) can be characterized by a conductance, $C_{BA}$ [$L^2T^{-1}$], such that the discharge, $Q_{BA}$, between the two zones can be expressed as

$$Q_{BA} = C_{BA}(h_B - h_A), \quad (3)$$

where $h_A$ is the head above the packer in borehole $A$ and $h_B$ is the head in borehole $B$. Each zone has a number of flow inlets and outlets that can be characterized individually by

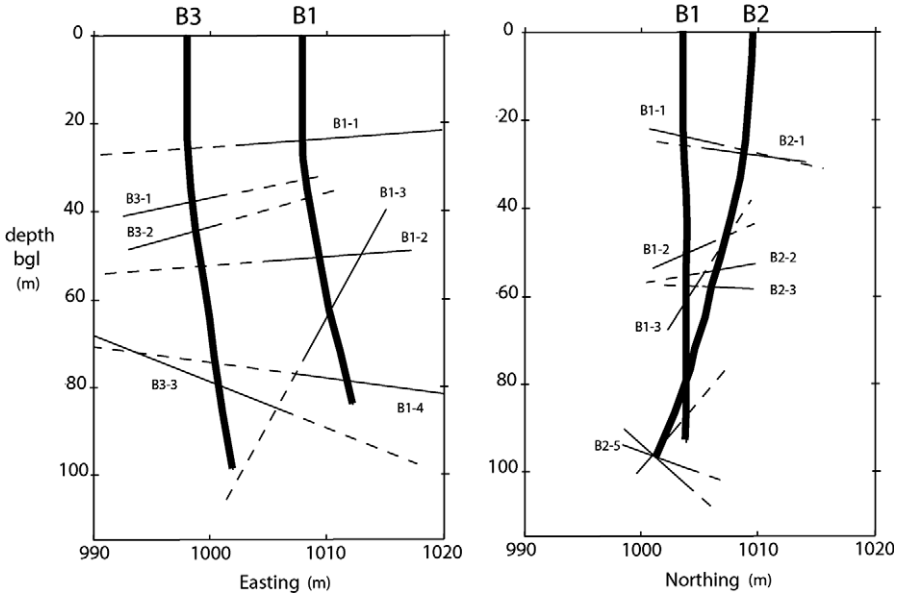


**Figure 4** Representation of the transmissive fractures in B3 and B1 (left) and B2 and B1 (right). Fracture traces are shown in the cross-section containing the two wells. Note that the boreholes are deviated from the vertical, but borehole B1 and B2 do not intersect: B1 is beside B2 (the minimum separation between the two boreholes is about 5 m) on the B1—B2 cross-section. The measured angles are corrected for the borehole deviations, which may be as high as 15° on this site.

a conductance, denoted by $C_{Ai}$ or $C_{Bi}$ and a fixed head, denoted by $H_{Ai}$ or $H_{Bi}$ (Fig. 5). To account for the ambient vertical flow observed in the boreholes at the site, the fixed heads are all allowed to be different. In the following, fixed heads, conductances and discharges relating to the pumped zone in borehole *A* have a subscript A and an integer subscript indicating the number of the inlet or outlet from the top of the borehole. Parameters relating to borehole *B* are defined similarly. The pumped zone in borehole *A* has *n* inlets and outlets and borehole *B* has *m* inlets and outlets

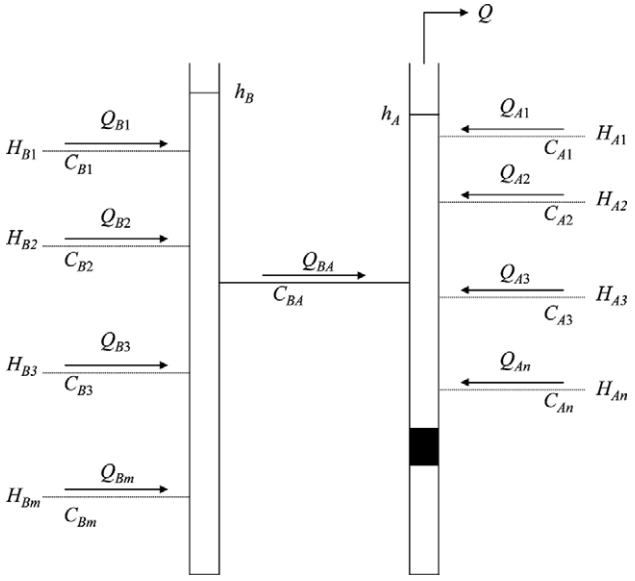


**Figure 5** Schematic representation of steady-state flows, conductances and fixed heads around boreholes *A* and *B* when the section of borehole *A* above the packer is pumped at a rate *Q*.

in addition to the flow pathway(s) characterized by $C_{BA}$. Other than the ordering of the inlets and outlets down each hole, no geometrical relationships are implied in Fig. 5.

The steady-state mass balance equations for boreholes *A* and *B* are

$$Q - Q_{BA} = \sum_{i=i}^{n} Q_{Ai} = \sum_{i=i}^{n} C_{Ai}(H_{Ai} - h_A) \tag{4}$$

and

$$Q_{BA} = \sum_{i=i}^{m} Q_{Bi} = \sum_{i=i}^{m} C_{Bi}(H_{Bi} - h_B). \tag{5}$$

Solving Eqs. (3)—(5) for $h_A$ gives

$$h_A = \frac{C_{BA}\left(\sum_{i=i}^{n} C_{Ai}H_{Ai} + \sum_{i=i}^{m} C_{Bi}H_{Bi}\right) + \left(\sum_{i=i}^{n} C_{Ai}H_{Ai}\right)\left(\sum_{i=i}^{m} C_{Bi}\right) - \left(C_{BA} + \sum_{i=i}^{m} C_{Bi}\right)Q}{C_{BA}\left(\sum_{i=i}^{n} C_{Ai} + \sum_{i=i}^{m} C_{Bi}\right) + \left(\sum_{i=i}^{n} C_{Ai}\right)\left(\sum_{i=i}^{m} C_{Bi}\right)} \tag{6}$$

and solving for $h_B$ gives

$$h_B = \frac{C_{BA}\left(\sum_{i=i}^{n} C_{Ai}H_{Ai} + \sum_{i=i}^{m} C_{Bi}H_{Bi}\right) + \left(\sum_{i=i}^{n} C_{Ai}\right)\left(\sum_{i=i}^{m} C_{Bi}H_{Bi}\right) - C_{BA}Q}{C_{BA}\left(\sum_{i=i}^{n} C_{Ai} + \sum_{i=i}^{m} C_{Bi}\right) + \left(\sum_{i=i}^{n} C_{Ai}\right)\left(\sum_{i=i}^{m} C_{Bi}\right)}. \tag{7}$$

The drawdown ($s_A$ and $s_B$ associated with $h_A$ and $h_B$, respectively) is given by the difference between the head when the pumping rate is zero and when it is *Q*. Thus,

$$s_A = \frac{\left(C_{BA} + \sum_{i=i}^{m} C_{Bi}\right)Q}{C_{BA}\left(\sum_{i=i}^{n} C_{Ai} + \sum_{i=i}^{m} C_{Bi}\right) + \left(\sum_{i=i}^{n} C_{Ai}\right)\left(\sum_{i=i}^{m} C_{Bi}\right)} \tag{8}$$

and

$$s_B = \frac{C_{BA}Q}{C_{BA}\left(\sum_{i=i}^{n} C_{Ai} + \sum_{i=i}^{m} C_{Bi}\right) + \left(\sum_{i=i}^{n} C_{Ai}\right)\left(\sum_{i=i}^{m} C_{Bi}\right)}. \quad (9)$$

Hence, dividing Eq. 9 by Eq. 8 gives

$$\frac{s_B}{s_A} = \frac{C_{BA}}{C_{BA} + \sum_{i=i}^{m} C_{Bi}} = \frac{C_{BA}}{C_B}, \quad (10)$$

where $C_B$ is the conductance characterizing steady-state converging flow to borehole *B* as defined in the section ''Single packer tests''. So the conductance between borehole *A* above packer and borehole *B* can be calculated from the tests simply by

$$C_{BA} = \frac{s_B}{s_A} C_B. \quad (11)$$

In the following, we assume that the conductance remains constant over the range of pumping rates used in the tests.

This approach to the analysis of the packer tests allows the connections between boreholes to be quantified without having to make assumptions of two-dimensional radial flow and the homogeneity of hydraulic properties, which are not well founded *a priori* in this study. Interconnections between fractures caused by the presence of the boreholes are automatically accounted for in the analysis. However, it should be noted that the packer also forms part of the tested system.

The conductance of the zone connecting the two boreholes is directly related to the drawdown ratio $s_{obs}/s_{pump}$ (Eq. 11). An illustration of this property is given in the appendix. Fig. A1 shows that for some simple connectivity patterns of two-dimensional fracture zones, the expected drawdown ratio $s_{obs}/s_{pump}$ may be solved explicitly. The analysis of the drawdown ratio $s_{obs}/s_{pump}$ as a function of the packer depths provides a direct information about fracture connectivity. An increase of $s_{obs}/s_{pump}$ as the packer is lowered indicates the presence of a fracture zone that is connected to the observation well (Fig. A1). Conversely, when the ratio $s_{obs}/s_{pump}$ remains constant as the packer is lowered, it indicates that the fracture zones at these depths are not connected to the observation well.

### Analysis of the fracture zone connectivity at the Stang er Brune site from single packer tests

Fig. 3 shows the cumulative conductance with depth in each borehole. The conductances describing steady-state converging flow to the open boreholes B1, B2 and B3 are 26, 192 and 442 $m^2d^{-1}$, respectively. The apparently anomalous result in B3 between 78.6 and 82.5 mbgl may be due to short-circuiting related to vertical hydraulic connectivity between the zones above and below the packer. Indeed the optical and acoustic logs show two high angle (85° dip) open features between 80 and 82 mbgl, but this was not investigated further in the field.

The hydraulic connections inferred from the analysis of single packer tests are synthesized in Fig. 7(a). In most cases, the transmissive zones are found to be either disconnected to the other boreholes or connected to all the other boreholes. This indicates the presence of fracture clusters that are well connected all over the site.

*Tests in borehole B1.* In borehole B1, hydraulic tests were conducted with the packer positioned at 33.3, 45.5, 52.1, 62.0 and 74.5 m and in the open hole (Fig. 6). From Fig. 6(b), it appears that there are three zones that connect with B3. Fig. 6(a) shows that the same zones connect with B2. These zones correspond to B1-1, B1-2 and B1-4. For the B1-4 zone, the interpretation in terms of connectivity is ambiguous, since the open borehole tests in Borehole 1 showed a relatively strong non-linear response even at the lowest pumping rate.

*Tests in borehole B2.* In borehole B2, single packer tests were carried out at 51.2, 55.2, 58.4, 61.0, 70.5, 81.0 and 83.0 m and in the open hole. Figs. 6(a) and (c) show that the zone above 51.2 m is relatively poorly connected to the other holes. The remaining tested sections of B2 all connect (to varying degrees) with B3. There is at most only a minor connection between the zones above 55.2 m and B1, and similarly little connection with B1 from the zone between 58.4 and 61.0 m. However, all other zones tested appear to connect with B1. It thus appears from single packer tests that the B2-2, B2-3, B2-4 and B2-5 fracture zones are connected to B1 and B3.

*Tests in borehole B3.* In borehole B3, hydraulic tests were done with the packer positioned at 41.5, 46.5, 48.5, 59.0, 79.1, 83.0 m and in the open hole. Figs. 6(b) and (c) show that the zones below 79.1 m and above 41.5 m connect with B1 and B2. Hence the B3-1, B3-2 and B3-3 fracture zones appear to be connected to B1 and B2.

## Cross-borehole flowmeter tests

Cross-borehole flowmeter tests are performed by turning on a pump in one of the wells, while monitoring changes in the vertical velocity in the other boreholes. This technique is based on the idea that changing the pumping conditions at a well will modify the head distribution in large-scale flow paths, which in turn should change the flow profiles in observation boreholes (Paillet, 1998; Williams and Paillet, 2002; Le Borgne et al., 2006a,b). Such cross-borehole flowmeter tests provide information on the properties of the flow zones that connect borehole pairs, whereas single-borehole flowmeter tests provide information about the properties of the individual fracture segments surrounding the borehole. The change in flow in observation wells induced by pumping in another well can be interpreted in terms of flow zone connectivity since the hydraulic head should change only in the flow paths connected to the pumping well. Cross-borehole tests were performed for three pairs of observation and pumping wells (Table 4). The full characterization of the fracture connectivity would have required performing flowmeter tests using each of the wells successively as pumping wells and observation wells. This was not done due to lack of time. The present dataset is however sufficient for the purpose of comparison with packer based techniques.

Fig. 8 shows an example of a cross-borehole flowmeter test. In this experiment, flow was measured as a function

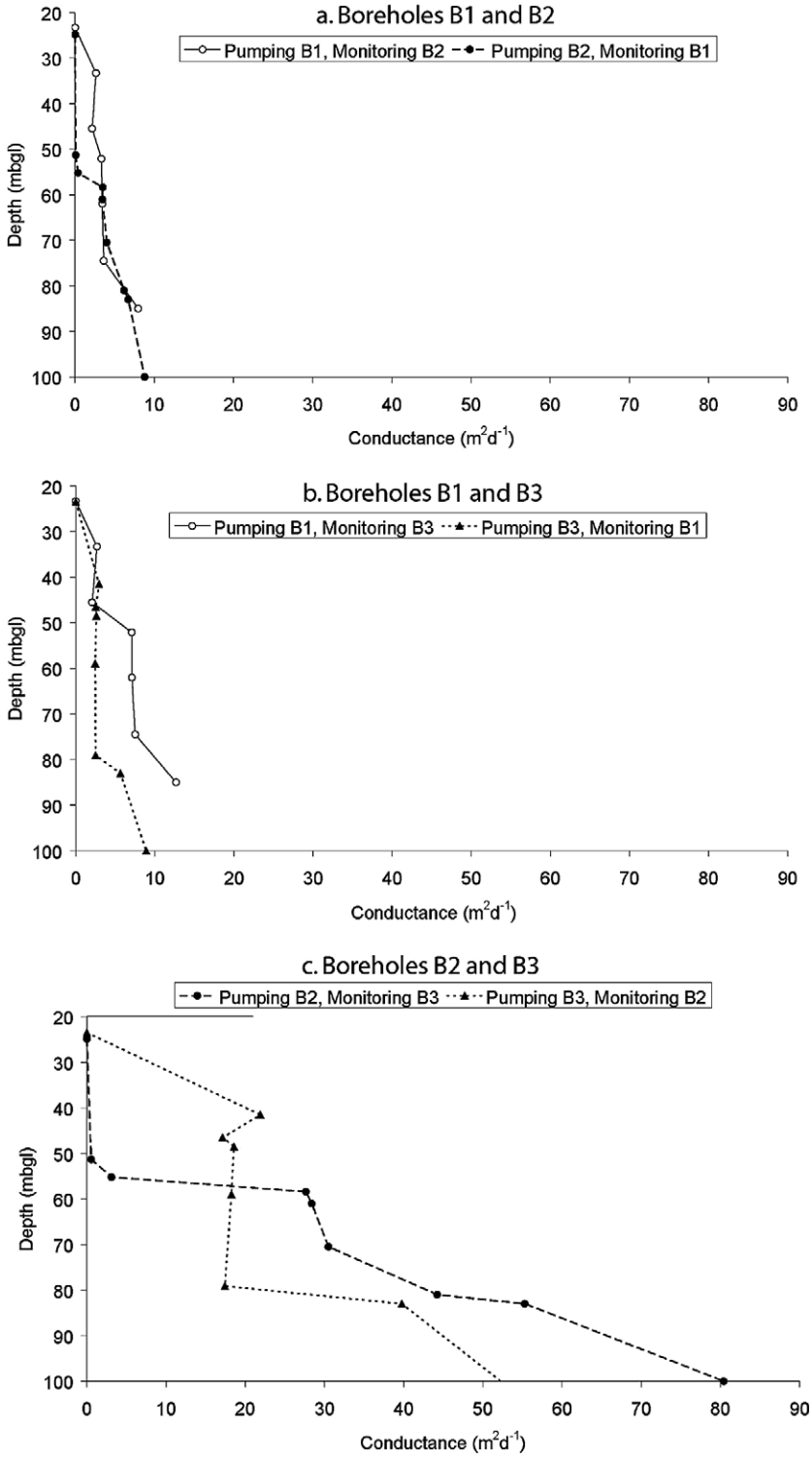


**Figure 6** Conductances between pairs of boreholes as a function of depth below ground level. Markers indicate the bottom of the packered zone in the pumped borehole. The top marker for each borehole indicates the location of the bottom of the casing.

of time at different depths in borehole B1, while a pump was turned on and off with 20 min cycles in an isolated interval of 80 cm (using a dual packer system) centred on the B3-2 fracture zone in borehole B3 (Fig. 8). The measured vertical flows at locations between and above the flow zones in borehole B1 are shown as the discrete data points in Fig. 8. Measurements at positions 3 and 4 show an increase in upflow followed by a return to ambient flow when the pump is turned off. On the other hand, flow measured at position 2 remains constant during the experiment except for a short decrease when the pump is started and a short increase when the pump is stopped. Such response is typical

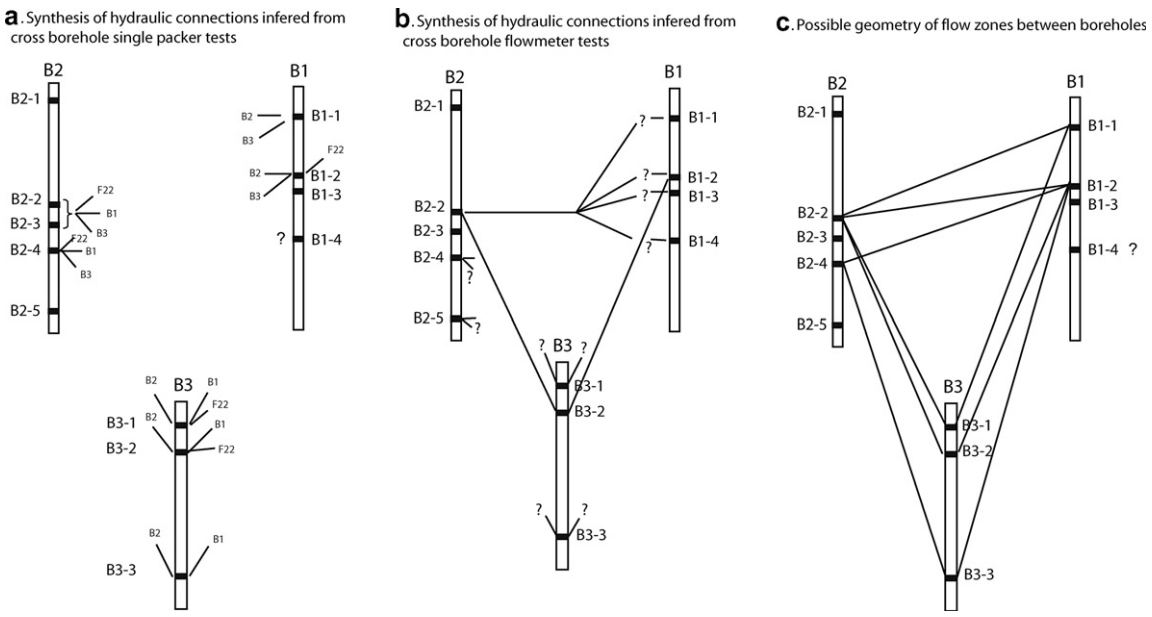


**Figure 7** (a) Synthesis of the hydraulic connections inferred from single packer tests. The connections with borehole F22 (Fig. 1) are also indicated. (b) Synthesis of the hydraulic connections determined from cross-borehole flowmeter tests. (c) Possible hydraulic connections at the Stang er Brune site inferred from the comparison of single packer tests and flowmeter tests results.

**Table 4** Cross-borehole flowmeter tests performed at the site

| Pumping zone | Observation well |
|---|---|
| B3-2 | B1 |
| B3-2 | B2 |
| B1 | B2 |

of flow resulting from the decrease or increase of borehole water level (also called borehole storage effect) (Lapcevic et al., 1993). Finally, the flow response above all flow zones (position 1) appears relatively noisy and difficult to correlate with pumping rate variations. The observed water level decreased to a minimum of about 3.5 cm and increased back towards the level measured at the start of the experiment when the pump is turned off.

The increase in upflow at positions 3 and 4 when the pump is turned on in the pumping well implies a decrease in hydraulic head in one of the flow zones above these depths. The fact that the flow remains constant at position 2 suggests that the zone where the hydraulic head is decreasing should be located between position 2 and 3. The only transmissive zone in this interval is the B1-2 fracture zone. Hence, it appears that when the pump is turned on in the isolated interval at 45 m depth in B3, the hydraulic head is decreasing in the B1-2 fracture zone. The fact that the flow measured at position 3 and 4 are nearly identical implies that the head in the B1-3 fracture zone does not change significantly during the experiment. The conclusion in term of connectivity is that the B3-2 zone in B3 is connected mainly to the B1-2 zone in B1.

The hydraulic connections inferred from all the cross-hole flowmeter tests are synthesized in Fig. 7(b). The cross-borehole flowmeter tests performed using B3 as a pumping well (with the B3-2 zone isolated with a double packer system) and B2 as observation well showed that the main head variation is occurring in the B2-2 fracture zone in B2. Another cross-borehole flowmeter test, with B1 as pumping well (the whole well was pumped) and B2 as observation well showed that the main head variation is occurring in the B2-2 fracture zone in B2 when pumping in B1. Flow was not measured between the B2-4 and B2-5 zones, so that the connectivity of the B2-4 zone cannot be assessed from this experiment. We can only conclude that one of these zones is not connected to the B1 well.

## Multi-level pressure monitoring

Cross-borehole flowmeter tests and single packer tests both agree that the B1-2 fracture zone in borehole B1 is connected to other boreholes (Fig. 7). To test the validity of this result, we isolated the B1-2 fracture zone in B1 with a double packer, and pumped borehole B3. Fig. 9 shows the evolution of hydraulic head when inflating the packers and when turning on a pump in borehole B3. First, the evolution of hydraulic head when inflating packers is a decrease of the hydraulic head above the packers of about 45 cm and a decrease of hydraulic head between packers of about 8 cm. The hydraulic head below the lower packer remains approximately constant. These differences in hydraulic head between the different fractures in the borehole are driving the measured ambient upward flow (Fig. 2(c)). When turning on the pump in borehole B3, the hydraulic head in the isolated interval in B1 decreased by about 5 cm, while the hydraulic heads on either side on the dual packer system remained constant. The same result was obtained when pumping in B2. Thus, the maximum head variation is observed in the B1-2 fracture zone when pumping other boreholes.

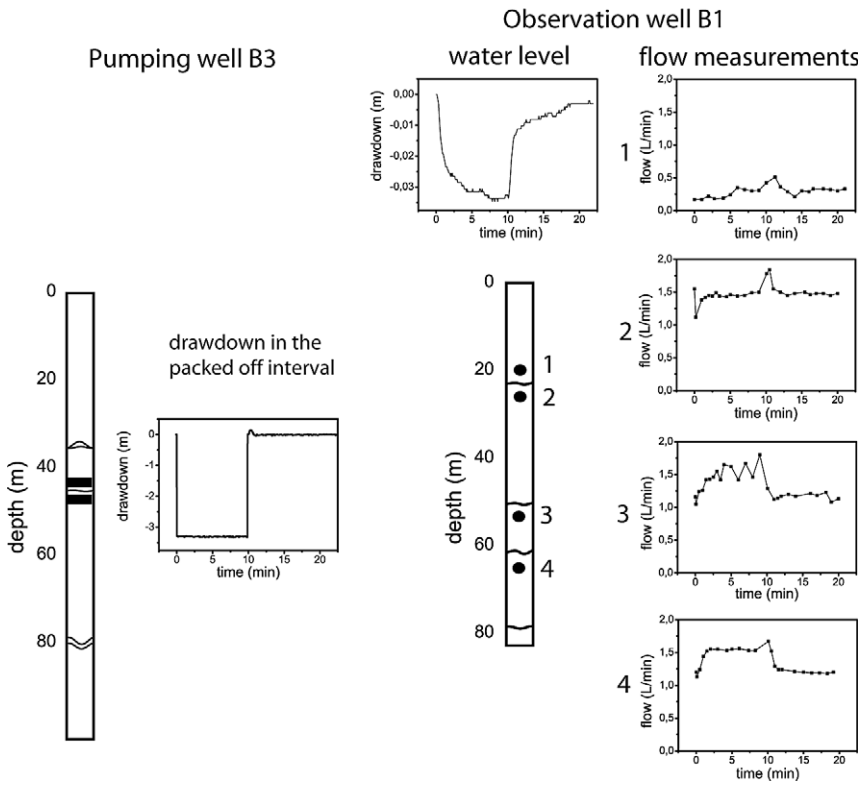


**Figure 8** Example of cross-hole flowmeter test. Vertical flow velocities are measured with the flowmeter stationed in borehole B1, while the pump is turned on in borehole B3 in a packered off interval (1 m length) at 45 m. The pump is turned off after 10 min. The experience is repeated with the flowmeter positioned at different depths (position 1: 21.6 m, position 2: 26 m, position 3: 52 m, position 4: 64 m).

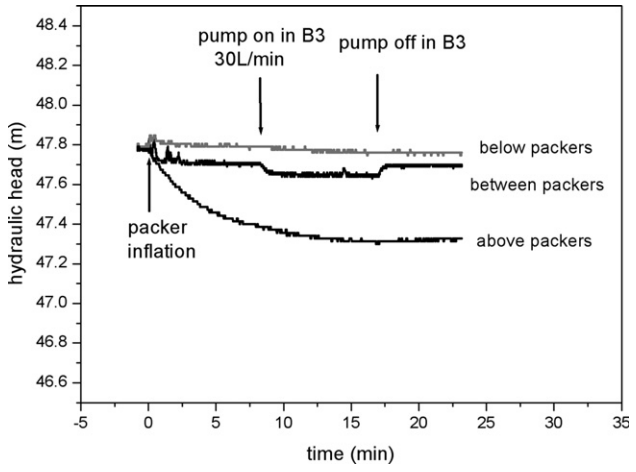


**Figure 9** Hydraulic head evolution between, above and below packers at 50.9 m in borehole B1, when inflating packers. The effect of turning on a pump in borehole B3 is to decrease the hydraulic head between packers whereas no significant responses are noticed above the top packer and below the lower packer.

The absence of a clear hydraulic response on either side of the dual packer system would appear to indicate that the B1-1 and B1-4 zones are not connected to the other boreholes. However, an alternative interpretation, for which there is some evidence from the single packer tests, is that the comparatively high drawdown in the packered interval occurs because the interval is relatively poorly connected hydraulically to its surroundings compared with its connection to B3. In addition, the low drawdown below the packered interval could quite reasonably be due to the fact that that section of the borehole is well connected to a transmissive network of fractures. Unfortunately, the existing evidence does not conclusively favour one of the interpretations. This illustrates the difficulty of characterizing connectivity by tracking hydraulic head variations, especially in the case that indirect connections exist.

## Synthesis on hydraulic connections

The characterization of fractures from borehole imaging and geophysical logging is obviously not sufficient to assess the geometry of flow structures, since the local properties of fractures may greatly differ from the properties of the main flow paths. On the other hand, single packer tests and cross-borehole flowmeter tests appear to be very complementary. By combining the results of single packer with flowmeter tests, we propose in Fig. 7(c) a geometry of the hydraulic connections at this site that is compatible with all the dataset obtained from the different techniques. Generally, the two methods provide consistent results. Note however that, in the case where multiple connections exist between boreholes, such as for borehole B2 and B3, it is difficult to determine exactly the pair of fractures that are

connected to each other, from either the flowmeter or the single packer methods. Obtaining such information requires the use of additional packers. This was done for two of the flowmeter experiments so that it was possible to assess one to one connections between fracture zones in the different boreholes (Fig. 7(b)). As we discussed in the section ''Tests in borehole B1'', the connectivity of the B1-4 zone with other boreholes is not clearly characterized from single packer tests due to quadratic head losses effects in the B1 well.

At the scale of the test site, the transmissive fractures are found to be well connected to each others. Nevertheless, none of them is found to intersect directly the other boreholes. The fracture network is composed of few of the fractures identified in the boreholes that form a connected cluster all over the site. The good connectivity of the fracture network is also observed on the main pumping site, where long-range hydraulic connections are belived to occur in the vicinity of the sub-horizontal contact between the intrusive granite and the overlying micaschist (Le Borgne et al., 2006a,b).

## Discussion and summary

As illustrated in this study, the characterization of fracture connectivity is difficult even for small-scale sites. On the test site, the connectivity of main transmissive zones was first assessed from single packer tests with pressure monitoring in adjacent wells. We showed that the analysis of the ratio of the drawdown in the observation well and the drawdown in the pumping for different packer positions allows an efficient characterization of the fracture zone connectivity. The comparison of these results with flowmeter test results showed that these different techniques provide relatively consistent results for characterizing the main connected flow zones. The permeable fracture network is composed of few of the fractures identified in the boreholes that form a connected cluster at the site scale.

Flowmeter and single packer tests provide a comparable level of information on connectivity. A limitation of the single packer technique is that it cannot be used in a screened borehole. In addition, two features of single packer testing need highlighting. First, vertical hydraulic connectivity between the zones above and below the packer produces a biased estimate of the conductance measured above the packer, which is indicated by an apparent reduction in conductance when the packer is lowered to below the short-circuiting fractures. Second, when drawdown in the observation hole is small, the measured conductance becomes sensitive to the drawdown measurement. This can occur when the packer is lowered through a transmissive region but the pumping rate has not been increased. The effect of this can be seen clearly in Fig. 6(c), which shows the open hole conductances between B2 and B3 to differ by nearly 30 $m^2$/day, whereas theoretically, these values should be identical. However, the drawdown in the observation holes is only 3 and 4 cm. A change of just 1 cm in either drawdown can reduce the difference in conductance to less than 10 $m^2$/day. Consequently, it is recommended that calculations of conductance be carried out following each test in the field so that short-circuiting can be identified (allowing further tests to be conducted to identify its cause), and so that the pumping rate can be adjusted where necessary to avoid oversensitivity of the measured conductances to observation hole drawdown.

The advantage of the flowmeter based method is that it does not require the use of packers and can be used in cased well. However, the interpretation of the cross-borehole flowmeter tests is less direct than that of single borehole packer tests. The use of flow measurement to characterize fracture connectivity implies interpreting the vertical flow variations in the borehole in terms of hydraulic head variations within each fracture zones. The interpretation of flow measurements allows to identify the zones where the largest hydraulic head variations occur when changing the pumping condition in a nearby well. The influence of the head variations in the fracture zones on the vertical flow in observation boreholes depends on the local transmissivity of these fracture zones in the boreholes. The consequence is that cross-borehole flowmeter tests will detect the most transmissive fracture among the fractures that are connected. Single packer tests do no have this limitation, at least for the upper fracture zones that can be isolated from the rest of the fractures.

The flowmeter tests are used to characterize which of the fracture zone in the observation well is connected to the pumping well, whereas single packer tests allow determining which of the fracture zone in the pumping well is connected to observation wells. The two methods are thus complementary. If multiple connections exist between boreholes, the distribution of connected fractures can be identified, but it is difficult to determine exactly to which fracture in the other boreholes they are connected. Obtaining such information requires some complementary dual packer tests, or more simply, to use in conjunction a single packer in the pumping well and a flowmeter in the observation well. The latter methodology should allow a much faster determination of preferential flow paths than the former one.

## Acknowledgements

This work was partly funded by the European projects ''ALIANCE'' (contract EVK1-CT-2001-00091) and SALTRANS (contract EVK1-CT-2000-00062). We also thank the CNRS for their financial support, through the INSUE project ''ORE H+'' and an ATIP project. The city of Plœmeur is also greatly thanked for its help for developing the site and during the experiments.

## Appendix. Illustration of the analysis of the drawdown ratio $s_{obs}/s_{pump}$ for some simple connectivity patterns

In order to illustrate the use of the method of interpretation of cross-borehole single packer tests, we consider some simple connectivity patterns and quantify the drawdown ratio $s_{obs}/s_{pump}$ for different packer positions in the pumping well (Fig. A1). The drawdown ratio $s_{obs}/s_{pump}$ is linearly related to the cross-borehole conductance (Eq. 11), which we use to characterize the cross-borehole connectivity (Fig. 6).

Three basic connectivity patterns are considered. Field situations are expected to be a combination of these cases. In case A, the pumping and observation well are connected through two fractures. In case B, one fracture is connected to the observation well and one fracture is disconnected. In case C, one fracture connects the pumping well and observation well and one disconnected fracture is present in both the observation and the pumping well. For each of these cases, we derived the expected drawdowns in the pumping well and the observation well, when the packer is between the fractures in the pumping well (position 1) and when the packer is below the fractures in the pumping well (position 2). We assumed that the fractures may be represented by homogeneous two-dimensional planes. We consider quasi-steady state conditions in a context with low storage coefficients and relatively large transmissivity implying that the pressure variations stabilize quickly. Note that this hypothesis may not be always met in natural systems. However, these simple examples are meant to be used as guidelines to interpret measurements in natural systems.

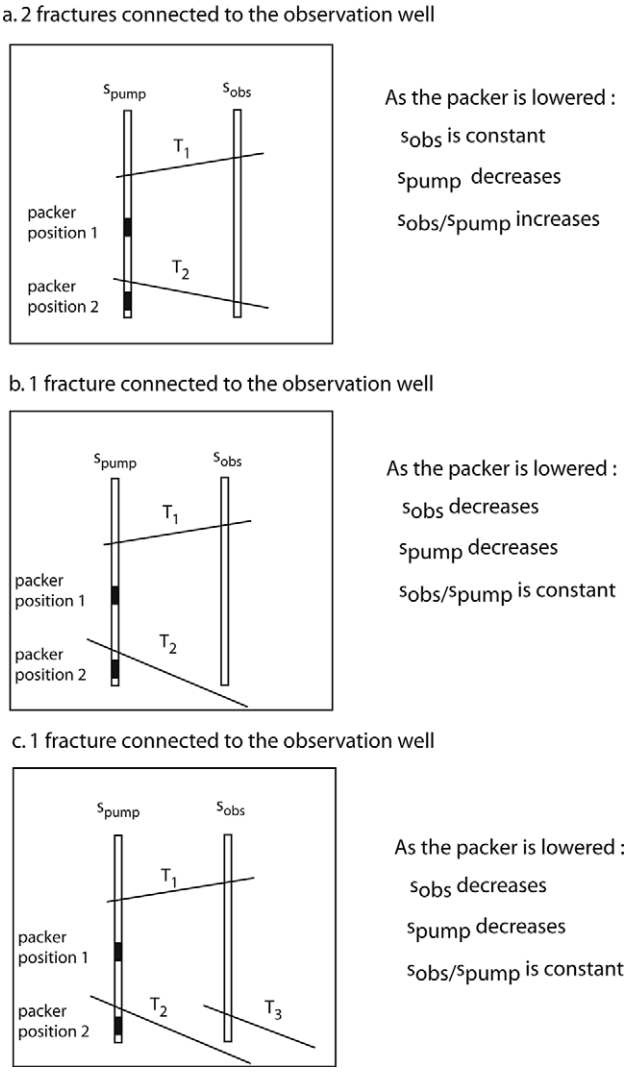


**Figure A1** Illustration of some simple connectivity configurations. For the different cases, we analyze the expected evolution of the drawdown in the pumping well and in the observation well as the packer is lowered in the pumping well. $s_{pump}$ is the quasi-steady state drawdown in the pumping well and $s_{obs}$ is the quasi-steady state drawdown in the observation well.

The main result of this analysis is that in the case where the two fractures are connected to the two boreholes, the drawdown in the observation remains constant as the packer is lowered. Hence, since the drawdown in the pumping well decreases as the packer is lowered, the drawdown ratio $s_{obs}/s_{pump}$ increases. In the cases where only one fracture is connected to the two wells (cases B and C), the drawdowns in the pumping and observation well decrease as the packer is lowered but the ratio $s_{obs}/s_{pump}$ is found to remain constant. The ratio $s_{obs}/s_{pump}$ is thus a direct indicator for characterizing fracture connectivity using cross-borehole single packer tests.

## Notations

| | |
|---|---|
| $s_{pump}$ | quasi-steady state drawdown in the pumping well |
| $s_{obs}$ | quasi-steady state drawdown in the observation well |
| $s_{obs1}$ | quasi-steady state drawdown in fracture 1 in the observation well created by the pumping in the pumping well |
| $s_{obs2}$ | quasi-steady state drawdown in fracture 2 in the observation well created by the pumping in the pumping well |
| $Q$ | flow rate pumped from the pumping well |
| $r_w$ | radius of the pumping well |
| $r$ | distance between the pumping and observation well |
| $r_\infty$ | radius of influence of the pumping well |

Note that the head variations expressed in this analysis are relative to possible existing ambient heads. Vertical flow in the observation wells is accounted for. The assumption that we make is that the flow in the borehole and the heads in the fracture zones are steady state. This is consistent with what we observe during the experiments. We consider that the radius of influence $r_\infty$ is the same for all the fractures. It depends on the hydraulic diffusivity of the fractures. Hence, some differences with these results are expected to occur in the field. However, in practice, the radius of influence appears within a logarithm in the equations. Thus, differences in radius of influences are not expected to impact dramatically the results.

## Case A

### Packer in position 1

$$s_{pump} = \frac{Q}{2\pi T_1} \ln(r_\infty / r_w),$$

$$s_{obs1} = \frac{Q}{2\pi T_1} \ln(r_\infty / r),$$

$$s_{obs2} = 0.$$

Due to vertical borehole flow between fractures, the drawdown in the observation well is given by the average of the drawdown in the fractures in the observation well, weighted by their relative transmissivity (Paillet, 1998).

$$s_{obs} = \frac{T_1 s_1 + T_2 s_2}{T_1 + T_2} = \frac{Q}{2\pi(T_1 + T_2)} \ln(r_\infty / r)$$

$$s_{obs}/s_{pump} = \frac{T_1}{T_1 + T_2} \frac{\ln(r_\infty / r)}{\ln(r_\infty / r_w)}.$$

**Packer in position 2**

$$s_{pump} = \frac{Q}{2\pi(T_1 + T_2)} \ln(r_\infty / r_w),$$

$$s_{obs1} = \frac{Q_1}{2\pi T_1} \ln(r_\infty / r),$$

$$s_{obs2} = \frac{Q_2}{2\pi T_2} \ln(r_\infty / r),$$

$$s_{obs} = \frac{Q}{2\pi(T_1 + T_2)} \ln(r_\infty / r),$$

$$s_{obs}/s_{pump} = \frac{\ln(r_\infty / r)}{\ln(r_\infty / r_w)}.$$

As the packer is lowered in the pumping well, the ratio $s_{obs}/s_{pump}$ increases.

## Case B

**Packer in position 1**

$$s_{pump} = \frac{Q}{2\pi T_1} \ln(r_\infty / r_w)$$

$$s_{obs} = \frac{Q}{2\pi T_1} \ln(r_\infty / r)$$

$$s_{obs}/s_{pump} = \frac{\ln(r_\infty / r)}{\ln(r_\infty / r_w)}.$$

**Packer in position 2**

As a first approximation, we consider that the flow pumped in the pumping well is divided proportionally to the fracture transmissivities (Molz et al., 1989):

$$\frac{Q_1}{T_1} = \frac{Q_2}{T_2} = \frac{Q}{T_1 + T_2}.$$

Note that this assumption has been discussed by Ruud and Kabala (1996).

$$s_{pump} = \frac{Q}{2\pi(T_1 + T_2)} \ln(r_\infty / r_w),$$

$$s_{obs} = \frac{Q_1}{2\pi T_1} \ln(r_\infty / r) = \frac{Q}{2\pi(T_1 + T_2)} \ln(r_\infty / r),$$

$$s_{obs}/s_{pump} = \frac{\ln(r_\infty / r)}{\ln(r_\infty / r_w)}.$$

As the packer is lowered in the pumping well, the ratios$_{obs}$/$s_{pump}$ remains constant.

## Case C

**Packer in position 1**

$$s_{pump} = \frac{Q}{2\pi T_1} \ln(r_\infty / r_w),$$

$$s_{obs1} = \frac{Q}{2\pi T_1} \ln(r_\infty / r),$$

$$s_{obs2} = 0,$$

$$s_{obs} = \frac{T_1 s_1 + T_3 s_3}{T_1 + T_3} = \frac{Q}{2\pi(T_1 + T_3)} \ln(r_\infty / r),$$

$$s_{obs}/s_{pump} = \frac{T_1}{T_1 + T_3} \frac{\ln(r_\infty / r)}{\ln(r_\infty / r_w)}.$$

**Packer in position 2**

$$s_{pump} = \frac{Q}{2\pi(T_1 + T_2)} \ln(r_\infty / r_w),$$

$$s_{obs1} = \frac{Q_1}{2\pi T_1} \ln(r_\infty / r),$$

$$s_{obs2} = 0,$$

$$s_{obs} = \frac{T_1 s_1 + T_3 s_3}{T_1 + T_3} = \frac{T_1}{T_1 + T_3} \frac{Q}{2\pi(T_1 + T_2)} \ln(r_\infty / r),$$

$$s_{obs}/s_{pump} = \frac{T_1}{T_1 + T_3} \frac{\ln(r_\infty / r)}{\ln(r_\infty / r_w)}.$$

As the packer is lowered in the pumping well, the ratios$_{obs}$/$s_{pump}$ remains constant.

## References


Bour, O., Davy, P., 1997. Connectivity of random fault networks following a power law fault length distribution. Water Resour. Res. 33, 1567–1583.

Butler, J.J., McElwee, C.D., Bohling, G.C., 1999. Pumping tests in networks of multilevel sampling wells: motivation and methodology. Water Resour. Res. 35 (11), 3553–3560.

Day-Lewis, F.D., Hsieh, P.A., Gorelick, S.M., 2000. Identifying fracture-zone geometry using simulated annealing and hydraulic connection data. Water Resour. Res. 36 (7), 1707–1721.

de Dreuzy, J.R., Davy, P., Bour, O., 2001a. Hydraulic properties of two-dimensional random fracture networks following a power law length distribution: 1-Effective connectivity. Water Resour. Res. 37 (8).

Dershowitz, W., Fidelibus, C., 1999. Derivation of equivalent pipe network analogues for 3D discrete fracture networks by the boundary element method. Water Resour. Res. 35 (9), 2685–2691.

Genter, A., Castaing, C., Dezayes, C., Tenzer, H., Traineau, H., villemin, T., 1997. Comparative analysis of direct (core) and indirect (borehole imaging tools) collection of fracture data in the Hot Dry rock soultz reservoir (France). J. Geophys. Res. 102 (B7), 15419–15431.

Hess, A.E., 1986. Identifying hydraulically conductive fractures with a slow velocity borehole flowmeter. Can. Geotechn. J. 23, 69–78.

Hitchmough, A.M., Riley, M.S., Herbert, A.W., Tellam, J.H., 2007. Estimating the hydraulic properties of the fracture network in a sandstone aquifer. J. Contamin. Hydrol. 93 (1–4), 38–57.

Hsieh, P.A., 1998. Scale effects in fluid flow through fractured geological media, Scale dependence and scale invariance in hydrology. Cambridge University Press, Cambridge, pp. 335–353.

Illman, W.A., 2006. Strong evidence of directional permeability scale effect in fractured rock. J. Hydrol. 319 (1–4), 227–236.

Karasaki, K., Freifeld, B., Cohen, A., Grossenbacher, K., Cook, P., Vasco, D., 2000. A multidisciplinary fractured rock characterization study at Raymond field site, Raymond, CA. J. Hydrol. 236, 17–34.

Kolditz, O., 2001. Non-linear flow in fractured rock. International Journal of Numerical Methods for Heat and Fluid Flow 11 (5–6), 547–575.

Lapcevic, P.A., Novakowski, K.S., Paillet, F.L., 1993. Analysis of flow in an observation well intersecting a single fracture. J. Hydrol. 151, 229–239.

Le Borgne, T., Paillet, F.L., Bour, O., Caudal, J.-P., 2006a. Cross borehole flowmeter tests for transient heads in heterogeneous aquifers. Ground Water 44 (3), 444–452.

Le Borgne, T., Bour, O., Paillet, F.L., Caudal, J.-P., 2006b. Assessment of preferential flow path connectivity and hydraulic properties at single-borehole and cross-borehole scales in a fractured aquifer. J. Hydrol. 2, 3–4.

Le Borgne, T., Bour, O., de Dreuzy, J.-R., Davy, P., Touchard, F., 2004. Equivalent mean flow models for fractured aquifers: insights from a pumping tests scaling interpretation. Water Resour. Res. 5. doi:10.1029/2003WR002436.

Lloyd, J.W., Greswell, R., Williams, G.M., Ward, R.S., Mackay, R., Riley, M.S., 1996. An integrated study of controls on solute transport in the Lincolnshire Limestone. Quarterly Journal of Engineering Geology 29 (4), 321–339.

Martinez-Landa, Carrera, 2006. A methodology to interpret cross-hole tests in a granite block. J. Hydrol. 325 (1–4), 222–240.

Molz, F.J., Morin, R.H., Hess, A.E., Melville, J.G., Güven, O., 1989. The impeller meter for measuring aquifer permeability variations: evaluation and comparison with other tests. Water Resour. Res. 25, 1677–1683.

Muldoon, M., Bradbury, K.R., 2005. Site characterization in densely fractured dolomite: comparison of methods. Ground Water 43 (6), 863–876.

Nativ, R., Adar, E., Assaf, L., Nygaard, E., 2003. Characterization of the hydraulic properties of fractures in chalk. Ground Water 41, 532–543.

Paillet, F.L., 1993. Using borehole geophysics and cross-borehole flow testing to define hydraulic connections between fracture zones in bedrock aquifers. J. Appl. Geophys. 30 (4), 261–279.

Paillet, F.L., 1998. Flow modelling and permeability estimations using borehole flow logs in heterogeneous fractured formations. Water Resour. Res. 34 (5), 997–1010.

Paillet, F.L., 2000. A field technique for estimating aquifer parameters using flow log data. Ground Water 38 (4), 510–521.

Paillet, F.L., 2004. Borehole flowmeter applications in irregular and large-diameter boreholes. J. Appl. Geophys. 55 (1-2), 39–59.

Pezard, P.A., Luthi, S.M., 1988. Borehole electrical images in the basement of the Cajon Pass Scientific Drillhole, California: fractures identification and tectonic implications. Geophys. Res. Lett. (15/9), 1017–1020.

Qian, J., Zhan, H., Zhao, W., Sun, F., 2005. Experimental study of turbulent unconfined flow in a single fracture. J. Hydrol. 311, 206–215.

Ruud, N.C., Kabala, Z.J., 1996. Numerical evaluation of flowmeter test interpretation methodologies. Water Resour. Res. 32 (4), 845–852.

Sanchez-Vila, X., Carrera, J., Girardi, J.P., 1996. Scale effects in transmissivity. J. Hydrol. 183 (1–2), 1–22.

Sanford, W.E., Cook, P.G., Robinson, N.I., Weatherill, D., 2006. Tracer mass recovery in fractured aquifers estimated from multiple well tests. Ground Water 44 (4), 564–573.

Williams, J.H., Paillet, F.L., 2002. Using flowmeter pulse tests to define hydraulic connections in the subsurface: a fractured shale example. J. Hydrol. 265 (8/30), 100–117.

Yeh, J., Liu, S., 2000. Hydraulic tomography: development of a new aquifer test method. Water Resour. Res. 36 (8), 2095–2106. doi:10.1029/2000WR900114.